Brillouin-scattering studies of the transverse acoustic modes of incommensurate K_2SeO_4

Gen Li, X.K. Chen, N.J. Tao,* and H.Z. Cummins
Department of Physics, City College, City University of New York, New York, New York 10031

R. M. Pick
Département de Recherches Physiques, Université Pierre et Marie Curie, 4 place Jussieu, 75230 Paris CEDEX 05, France

G. Hauret
Laboratoire d'Etudes Physiques des Materiaux, Centre de Recherches sur la Physique des Hautes Températures, Université d'Orleans, Boîte Postale 6759, 45067 Orleans CEDEX, France
(Received 3 April 1991)

Brillouin scattering from the six pure transverse acoustic modes of K_2SeO_4 from 80 to 300 K was investigated. The temperature dependence of the hypersonic shear elastic constants C_{44}, C_{55} and C_{66} and the corresponding damping constants were obtained. C_{44} and C_{66} show anomalies near T_i and C_{55} near T_c, closely resembling the results of ultrasonic experiments. The C_{44} anomaly was analyzed in terms of bilinear coupling to the lowest temperature-dependent B_{3g} optical mode, which was observed in Raman scattering. The C_{55} anomaly near T_c was compared with the plane-wave-approximation result for the coupling of the strain to the phason. For the three pairs of transverse acoustic modes there was no asymmetry observed in the incommensurate and commensurate phases under interchange of the propagation and polarization directions.

I. INTRODUCTION

Brillouin scattering studies of K_2SeO_4 near the incommensurate ($T_i \sim 129$ K) and commensurate ($T_c \sim 94$ K) phase transitions have been reported by several groups.[1–6] However, attempts to observe Brillouin scattering from the pure transverse acoustic modes were not successful because the Brillouin-scattering intensities are extremely weak. By exploiting the high contrast and high resolution of a six-pass (2×3) Sandercock tandem Fabry-Perot interferometer, we were able to observe and study the weak Brillouin scattering from the pure transverse acoustic modes of K_2SeO_4.

The transverse elastic anomalies of K_2SeO_4 have been studied by Rehwald *et al.*[3,7] with ultrasonic techniques. The C_{44} elastic constant exhibits anomalies in the normal and incommensurate phases in which the elastic constant decreases when the temperature approaches T_i from either side. The C_{55} elastic constant exhibits a major decrease when the temperature approaches T_c in the incommensurate phase. Rehwald *et al.*[3] also determined the hypersonic shear elastic constants indirectly by using Brillouin-scattering results from quasilongitudinal and quasitransverse modes.

A C_{44} elastic anomaly similar to that in K_2SeO_4 was observed in the isomorph Rb_2ZnCl_4.[8,9] An explanation of the Rb_2ZnCl_4 C_{44} anomaly in the normal phase was proposed by Hirotsu *et al.*[8] based on an assumed bilinear coupling of the strain ε_4 with the zone-center mode of the soft Σ_2 branch. Neutron-scattering studies[10] of K_2SeO_4 indicated that the softening of the Σ_2 branch at q_0 extends to the zone-center mode, which also softens with decreasing temperature in the normal phase, decreasing to ~ 20 cm^{-1} at T_i. Because the C_{44} transverse acoustic mode at $q \sim 0$ belongs to the B_{3g} representation in the normal phase ($Pnam$), the bilinear coupling assumption can work only if the zone-center mode on the Σ_2 branch also belongs to the B_{3g} representation. Compatibility indicates that it may belong to either the B_{3g} or A_u representation;[10] however, previous Raman-scattering studies[11,12] and our Raman-scattering experiments described below have not revealed this zone center mode (~ 25 cm^{-1} at room temperature). Furthermore, theoretical simulation results[13] indicated that the symmetry of the zone center mode on the soft Σ_2 branch belongs to the Raman-inactive A_u representation, rather than B_{3g}, which is Raman active. Therefore, the assumption of bilinear coupling of the C_{44} acoustic mode with the zone-center mode on the Σ_2 soft branch seems unlikely (although it may be possible that the mode actually is of B_{3g} symmetry but has an extremely small Raman cross section).

We propose that the C_{44} elastic anomaly results from bilinear coupling of the ε_4 strain to the lowest frequency B_{3g} optical mode which is *not*, however, on the soft Σ_2 branch. Previous Raman scattering studies[11] showed that the lowest-frequency B_{3g} optical mode (~ 50 cm^{-1}) exhibits partial softening in the normal phase. We also performed Raman-scattering measurements to study the temperature dependence of this B_{3g} mode, and we found that the temperature dependence of its frequency (Ω_B) is very similar to that of the C_{44} elastic constant. Leaving aside the origin of the temperature dependence of this B_{3g} mode and considering its interaction with the C_{44} acoustic mode, we can then explain the C_{44} anomaly in the normal phase.

Several theoretical analyses have predicted asymmetries for the velocity or attenuation of transverse sound waves in incommensurately modulated crystals under interchange of propagation and polarization directions due to the coupling effect with the phase mode in the incommensurate phase. Experimental observations of such asymmetries have been reported in $BaMnF_4$,[14] $RbH_3(SeO_3)_2$,[15] and quartz.[16] To investigate these transverse acoustic asymmetries in K_2SeO_4, we studied the Brillouin spectra of all six pure transverse acoustic modes in the normal, incommensurate, and commensurate phases.

II. EXPERIMENTS

A. Brillouin scattering

Our Brillouin-scattering apparatus, which is based on a Sandercock tandem Fabry-Pérot interferometer, has been described in a previous publication.[6] All measurements were performed in a 90° depolarized (VH) scattering geometry. The Spectra Physics argon ion laser was operated at 4880 Å with single-mode output power of $\sim$ 250 mW. Due to the weakness of the Brillouin-scattering intensity of the transverse acoustic modes, each spectrum was obtained with a long collection time (from 1/2 to 10 h). The preparation of the K_2SeO_4 crystals and the sample cooling system were also described in the previous publication.[6] To investigate all six transverse modes with wave vectors along the crystal axes, three samples with different orientations were used. The size of the samples was about 6 mm on each side. They were cut so that each crystal has two faces perpendicular to a different crystal axis (a, b, or c) and the four other faces perpendicular to the bisectors of the other two crystal axes.

B. Raman scattering

To investigate the lowest B_{3g} optical mode, Raman-scattering studies were performed from room temperature to liquid N_2 temperature. The conventional Raman-scattering apparatus has been described previously.[17] The K_2SeO_4 crystal used in the Raman-scattering experiment was cut with its faces perpendicular to the crystal axes and was also about 6 mm on each side. Spectra were collected in the 90° $b(c,b)a$ scattering geometry.

III. RESULTS

A. Brillouin scattering

Brillouin scattering from the transverse acoustic modes was investigated in the temperature range from 300 K (440 K for the C_{44} mode) to 80 K. Figure 1 shows two room-temperature 90° Brillouin-scattering spectra of K_2SeO_4 obtained in the scattering geometries of (a): $(b-c)[a,T](b+c)$ and (b): $(b-c)[a,b-c](b+c)$. The strong LA components in the (VT) spectrum (a) correspond to the C_{33} longitudinal mode, and the weak TA components correspond to the C_{55} transverse mode. In the (VH) depolarized spectrum (b), the LA components are eliminated (except for the $\sim$ 1% leakage from the imperfect polarizer) while the TA components are shown clearly. The shear elastic constants C_{ii} and linewidths

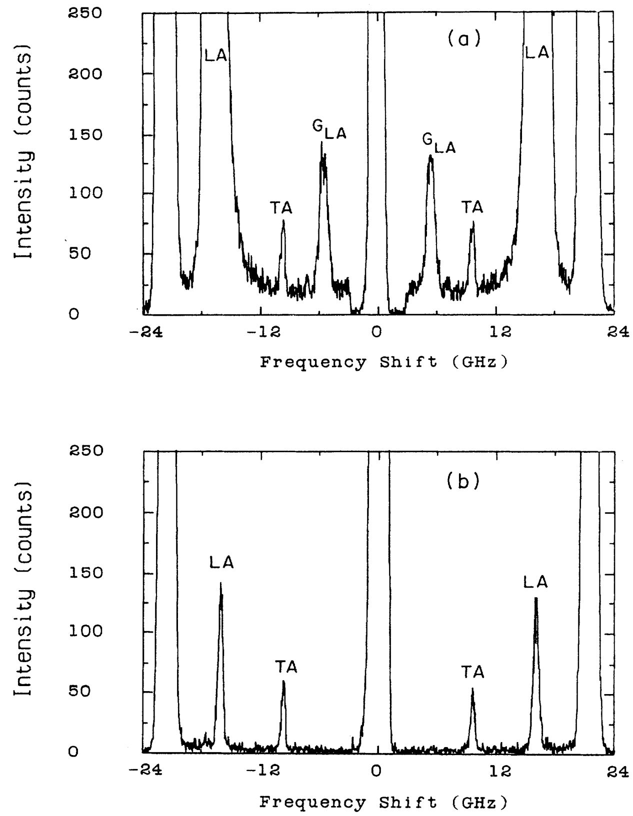

FIG. 1. Room-temperature 90° Brillouin-scattering spectra of K_2SeO_4 in the scattering geometries of: (a) $(b-c)[a,T](b+c)$; (b) $(b-c)[a,b-c](b+c)$. The features labeled LA, TA, and G_{LA} are the longitudinal modes, transverse modes, and the ghosts (neighboring order) of the LA components, respectively. The LA components in (b) are due to leakage.

γ_{ii} $(i = 4,5,6)$ were obtained by fitting the Brillouin components to a damped-harmonic-oscillator function:

$$S(\omega) = \frac{k_B T}{\omega}\frac{\omega\gamma_{ii}}{(\omega^2-\omega_0^2)^2+\omega^2\gamma_{ii}^2} \tag{1}$$

after deconvoluting the instrument function. In obtaining the C_{ii} we used

$$C_{ii} = \frac{\rho_m}{2(n_I^2+n_S^2)}\left(\frac{\Delta\nu_i\lambda_0}{\sin(\theta/2)}\right)^2, \tag{2}$$

where ρ_m is the density, n_I and n_S the refractive indices for the incident and scatted light, respectively, $\Delta\nu_i = \omega_0/2\pi$ is the Brillouin frequency shift in Hz, and λ_0 the vacuum wavelength of the laser light in cm. Experimental results[18] show that in the temperature range of interest, the density varies by $\leq$ 1.5% and this variation may be partially compensated by the variation of the refractive indices. Therefore the room-temperature values of ρ_m=3.05 g cm^{-3}, $n_a = 1.549$, $n_b = 1.539$, and $n_c = 1.543$ were used in the calculations.

Figures 2 and 3 show the temperature dependences of the elastic constants C_{ii} $(i = 4,5,6)$ in GPa (1

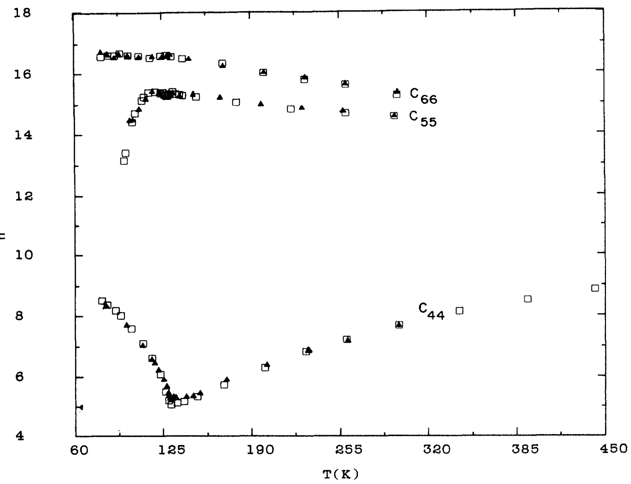

FIG. 2. Temperature dependence of the shear elastic constants C_{ii} from 90° Brillouin-scattering data. The corresponding transverse modes are represented by the following: for C_{44}, squares—($\mathbf{q} \parallel b$, $\mathbf{u} \parallel c$), triangles—($\mathbf{q} \parallel c$, $\mathbf{u} \parallel b$); for C_{55}, squares—($\mathbf{q} \parallel a$, $\mathbf{u} \parallel c$), triangles—($\mathbf{q} \parallel c$, $\mathbf{u} \parallel a$); for C_{66}, squares—($\mathbf{q} \parallel a$, $\mathbf{u} \parallel b$), triangles—($\mathbf{q} \parallel b$, $\mathbf{u} \parallel a$).

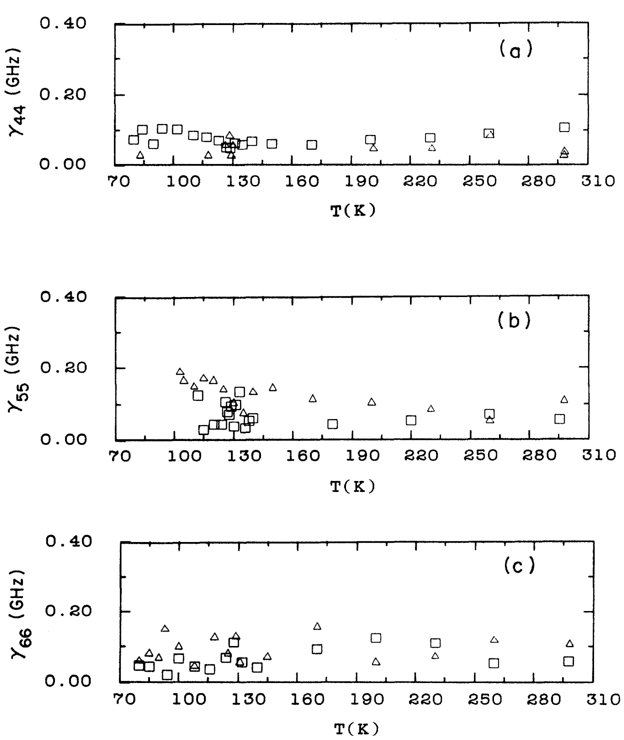

FIG. 3. Temperature dependence of the transverse mode damping constants γ_{ii} from 90° Brillouin-scattering spectra. The corresponding transverse modes are represented by (a) γ_{44}, squares—($\mathbf{q} \parallel b$, $\mathbf{u} \parallel c$), triangles—($\mathbf{q} \parallel c$, $\mathbf{u} \parallel b$); (b) γ_{55}, squares—($\mathbf{q} \parallel a$, $\mathbf{u} \parallel c$), triangles—($\mathbf{q} \parallel c$, $\mathbf{u} \parallel a$); (c) γ_{66}, squares—($\mathbf{q} \parallel a$, $\mathbf{u} \parallel b$), triangles—($\mathbf{q} \parallel b$, $\mathbf{u} \parallel a$).

GPa=1×10^{10} dyn/cm^2) and damping constants γ_{ii} ($i = 4, 5, 6$) deduced from the Brillouin spectra of the six transverse acoustic modes via Eqs. (1) and (2). For C_{44} and γ_{44}, squares represent the results of the transverse mode propagating along the b direction and polarized along the c direction ($\mathbf{q} \parallel b$, $\mathbf{u} \parallel c$) and triangles represent the results with ($\mathbf{q} \parallel c$, $\mathbf{u} \parallel b$), with interchanged $\mathbf{q}$ and $\mathbf{u}$ directions from the squares. In the same way, we denote the results for the two C_{55} modes with squares ($\mathbf{q} \parallel a$, $\mathbf{u} \parallel c$) and triangles ($\mathbf{q} \parallel c$, $\mathbf{u} \parallel a$); and for the C_{66} modes with squares ($\mathbf{q} \parallel a$, $\mathbf{u} \parallel b$), and triangles ($\mathbf{q} \parallel b$, $\mathbf{u} \parallel a$). When the temperature approached T_c in the incommensurate phase, the Brillouin intensity of the C_{55} modes decreased dramatically, making further low-temperature measurements impossible.

The weakness of the transverse Brillouin modes caused relatively large uncertainties in determining the frequency shifts and damping constants. The accuracies for the elastic constants and attenuations are estimated as ~ 0.3 GPa and ~ 100 MHz, respectively, around room temperature, and ~ 0.6 GPa and ~ 200 MHz at low temperatures. It can be seen from Figs. 2 and 3 that within the experimental accuracy there is no observable asymmetry in the C_{ii} and γ_{ii} for the pairs of transverse modes under interchange of propagation and polarization directions.

A comparison of our hypersonic shear elastic constants C_{44}, C_{55}, and C_{66} with the results of Rehwald *et al.*[3] shows that our results are similar to their ultrasonic results, but somewhat different from their hypersonic results, which were obtained indirectly from Brillouin results for QL and QT mixed modes.

Of the measured shear elastic constants, only C_{44} shows pronounced variations around T_i with a gradual decrease of about 40% when the temperature approaches T_i from either side. Only C_{55} shows an anomaly near T_c with a significant decrease when the temperature approaches T_c in the incommensurate phase. Of all the measured damping constants, no anomaly was observed within our experimental accuracy.

Figure 4 shows the temperature dependence of the integrated Brillouin-scattering intensities (I_{44}, I_{55}, and I_{66}) of the C_{44}, C_{55}, and C_{66} transverse modes. They were obtained by integration over the area of the corresponding Brillouin components and normalization with the laser power and the collection time. The accuracy of these values is estimated to be $\sim 20\%$. As shown in Fig. 4, the Brillouin intensity I_{44} of the C_{44} mode exhibits anomalous increases on both sides of T_i, while I_{55} decreases rapidly to zero as T approaches T_c.

B. Raman scattering

Figure 5 shows three Raman spectra of the lowest B_{3g} optical mode at 295, 130, and 78 K. It is clear from the first two spectra that no B_{3g} Raman mode was observed around 25 cm^{-1}, which is the frequency of the zone center mode on the soft Σ_2 branch found in inelastic-neutron-scattering experiments.[10] The weak mode seen in the last

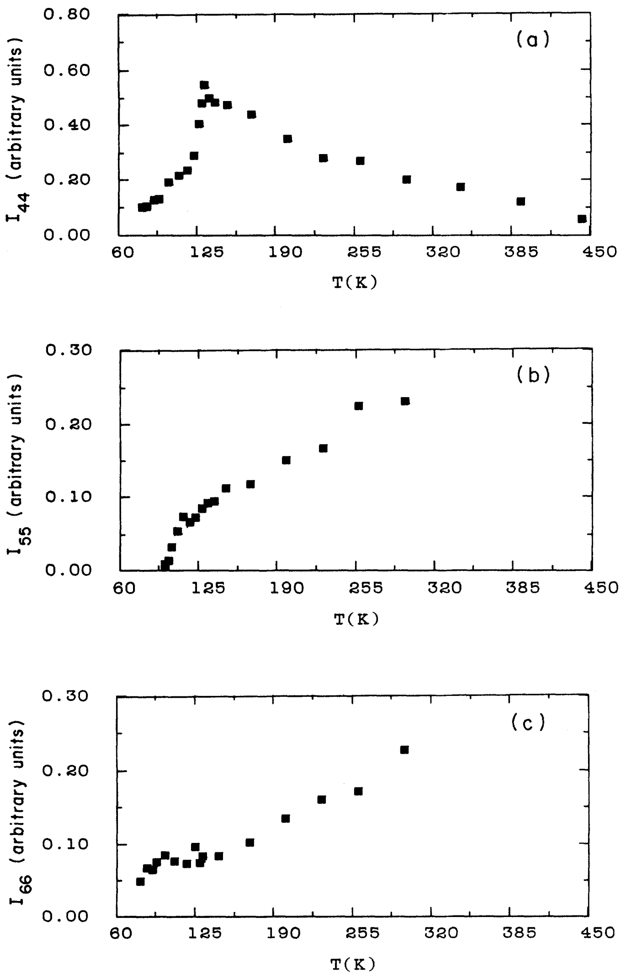

FIG. 4. Temperature dependence of the integrated Brillouin-scattering intensities: (a) C_{44} transverse mode—I_{44}; (b) C_{55} transverse mode—I_{55}; and (c) C_{66} transverse mode—I_{66} (in arbitrary units).

spectrum at 27 cm^{-1} is a zone-folded mode which has been discussed previously.[17,19] From the peak position of the B_{3g} Raman mode near 50 cm^{-1}, we obtained the temperature dependence of the frequency $\Omega_B(T)$ as shown in Fig. 6. The variation of $\Omega_B(T)$ with temperature is well represented by

$$\Omega_B^2(T) = [8.8(T - T_i)^{0.83} + 2.1 \times 10^2]\ (\text{cm}^{-1})^2 \quad (T > T_i), \quad (3)$$

$$\Omega_B^2(T) = [52(T_i - T)^{0.60} + 2.1 \times 10^2]\ (\text{cm}^{-1})^2 \quad (T < T_i), \quad (4)$$

as shown by the solid lines in Fig. 6, with $T_i = 129.5$ K.

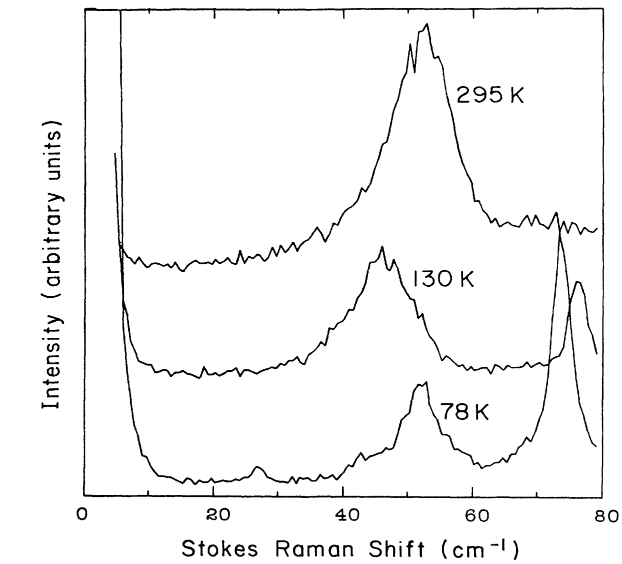

FIG. 5. Raman-scattering spectra of K_2SeO_4 at 295, 130, and 78 K in the $b(c,b)a$ scattering geometry, showing the temperature dependence of the lowest B_{3g} optical mode.

IV. ANALYSIS AND DISCUSSIONS

A. C_{44} elastic anomaly

1. *Theory*

The anomalies of the C_{44} elastic constant and the I_{44} Brillouin-scattering intensity in the normal phase indicate a bilinear interaction between the strain ε_4 and a zone-center ordering quantity with the same symmetry as ε_4. For the reasons discussed above, we will consider the lowest B_{3g} optical mode as the ordering quantity and carry out an analysis of the C_{44} elastic anomaly.

The standard phenomenological coupled-mode analysis for an acoustic mode (strain ε_4, with uncoupled elastic constant C_{44}^0 and damping constant γ_{44}^0) coupled to an

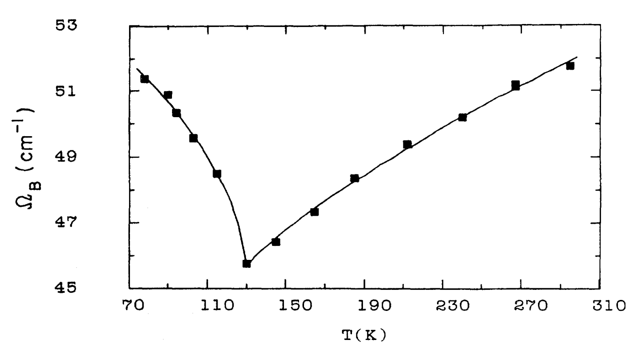

FIG. 6. Temperature dependence of the lowest B_{3g} optical mode frequency. Solid lines are the fitted results given by Eqs. (3) and(4).

optic mode (amplitude Q_B, frequency Ω_B, damping constant Γ_B) through a bilinear interaction ($a_4 Q_B \varepsilon_4$) leads to a predicted elastic constant C_{44} and damping constant γ_{44} for $T > T_i$ of

$$C_{44}(T) = C_{44}^0 - \frac{a_4^2}{\Omega_B^2(T)} \quad (T > T_i), \tag{5}$$

$$\gamma_{44}(T) = \gamma_{44}^0 + \frac{q^2}{\rho_m} \frac{a_4^2 \Gamma_B}{\Omega_B^4(T)} \quad (T > T_i), \tag{6}$$

where we have used the fact that $\Omega_B >> \omega$ or Γ_B to eliminate terms in ω^2 and $\omega\Gamma_B$. Equation (5) is the well-known static bilinear coupling result which has been discussed by many authors.[20–22] It predicts that the decrease of $\Omega_B(T)$ will cause a decrease of the C_{44} elastic constant, providing a possible explanation for the C_{44} elastic anomaly in the normal phase.

In the incommensurate and commensurate phases, the C_{44} acoustic mode still can couple bilinearly with the same zone-center optical mode as in the normal phase because both modes still have the same symmetry and belong to the B_2 representation in the commensurate phase. However, in the incommensurate and commensurate phases, the C_{44} acoustic mode also can couple to the modulation wave through a quartic coupling term $g_4 \rho^2 \varepsilon_4^2$ in which g_4 is a constant and ρ is the amplitude of the modulation wave which is the condensed soft mode on the Σ_2 branch. This coupling will lead to an additional modification of C_{44} given by

$$\Delta C_{44} = 2 g_4 \rho_0^2, \tag{7}$$

where ρ_0 is the equilibrium value of the order parameter. A mean-field evaluation of ρ_0 has been given previously.[6] The C_{44} elastic constant below T_i is then given by

$$C_{44}(T) = C_{44}^0 - \frac{a_4^2}{\Omega_B^2(T)} + 2 g_4 \rho_0^2 \quad (T < T_i). \tag{8}$$

Equations (5) and (8) together describe the temperature variations of the C_{44} elastic constant in the high-temperature normal phase and the low-temperature incommensurate and commensurate phases.

2. Comparison with experiment

To compare Eqs. (5), (6), and (8) with our experimental results, we first fitted Eq. (5) to the C_{44} data in the normal phase ($T > T_i$) with C_{44}^0 and a_4 treated as adjustable parameters and $\Omega_B^2(T)$ given by Eq. (3). The best fit was obtained with C_{44}^0=17 GPa and a_4 = 3.0×10^{18} $g^{1/2}\,cm^{-1/2}\,s^{-2}$. Keeping these values of C_{44}^0 and a_4 fixed, we then fit Eq. (8) to the low-temperature ($T < T_i$) C_{44} data with g_4 as the only adjustable parameter. $\Omega_B^2(T)$ was determined from Eq. (4), while ρ_0^2 was again determined by the mean-field results.[6] We obtained the best fit with $g_4 = 1.8 \times 10^{27}$ s^{-2}. Figure 7 shows the comparison of the calculated results of Eqs. (5) and (8) with the experimental results. The dotted line in the low-temperature phases ($T < T_i$) indicates the contribution from the first two terms of Eq. (8) and the solid lines are the total contributions. The agreement between the theory and the C_{44} data is excellent, except for the region very close to T_i where some rounding is observed in the data.

The predicted anomaly of the damping constant γ_{44} due to the bilinear coupling can be estimated by using

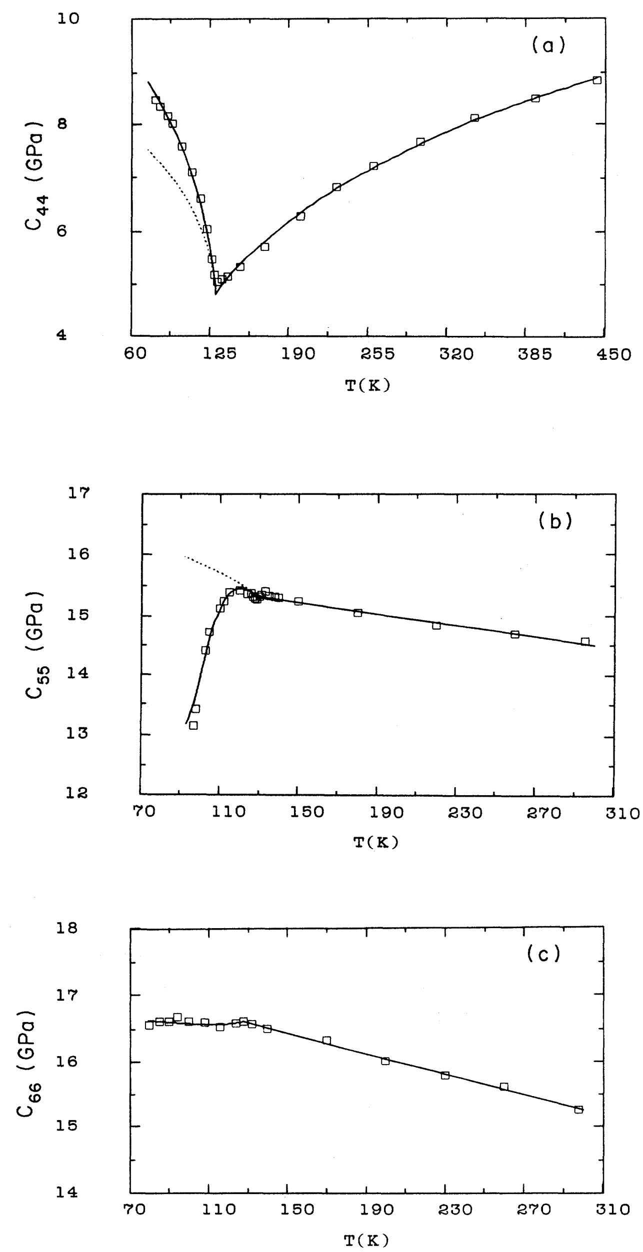

FIG. 7. Comparison of the experimental (a) C_{44}, (b) C_{55}, and (c) C_{66} data (squares) with the best-fit results (solid lines) of Eqs. (5) and (8), Eq. (13), and Eq. (15), respectively. The dotted line for C_{44} in the low-temperature phases ($T < T_i$) is the result of the first two terms in Eq. (8), showing the contribution of the bilinear coupling in the low-temperature phases, and the dotted line for C_{55} below T_i is the result of the first two terms in Eq. (13).

Eq. (6). With $q = 2.8 \times 10^5$ cm^{-1}(90° scattering and $\lambda_{\rm laser} = 488$ nm), $\Gamma_B \simeq 300$ GHz, and the above fitted a_4 value, we found that the maximum variation of $\gamma_{44}(T)$ is $(\Delta\gamma_{44})_{\rm max} \simeq 13$ MHz. Such a small variation is beyond our experimental accuracy, which explains why the damping anomaly is not observed in our measured attenuation results shown in Fig. 3.

Because K_2SeO_4 belongs to the universality class of the three-dimensional (3D) XY model for which $2\beta = 0.691$,[23,24] an analysis of the low-temperature ($T < T_i$) C_{44} data using Eq. (8) with a non-mean-field $\rho_0 \propto (T_i - T)^\beta$ was also attempted with β as a free parameter. The fits with mean field or with $2\beta = 0.70$ were found to be equally good. We note that Chen[25] has recently shown that the specific-heat anomalies of both K_2SeO_4 and Rb_2ZnCl_4 are consistent with the predictions of the 3D XY model.

3. Comparison with previous studies

The C_{44} elastic anomaly of K_2SeO_4 and the isomorph Rb_2ZnCl_4 were previously investigated by several groups. Hirotsu *et al.*[8] were the first to observe the C_{44} anomaly of Rb_2ZnCl_4 around the normal-incommensurate phase transition by ultrasonic measurements. Noting the considerable decrease of C_{44} with decreasing temperature in the normal phase, they suggested a possible explanation of bilinear coupling of the C_{44} acoustic mode with the zone-center mode on the soft Σ_2 branch, providing that there was also a soft Σ_2 branch in Rb_2ZnCl_4 like that in K_2SeO_4 and that the zone-center mode on the branch belonged to the B_{3g} (rather than A_u) representation. We note, however, that neutron-scattering studies of Rb_2ZnCl_4 have *not* shown a soft Σ_2 branch, and a theoretical study by Katkanant *et al.*[26] indicated that in Rb_2ZnCl_4 the incommensurate transition is entropy driven and shows no soft-mode behavior.

Rehwald *et al.*[3] reported a complete study of the elastic constants of K_2SeO_4 combining ultrasonic and Brillouin-scattering results. Following Hirotsu's suggestion, they assumed that the temperature dependence of $C_{44}(T)$ results from bilinear coupling to the zone-center mode on the Σ_2 soft branch. Representing the frequency of this mode as $\Omega^2 = b(T - T_0^e)$ and denoting the temperature at which $C_{44}(T)$ extrapolates to zero as T_0^σ they derived an elastic Curie-Weiss law for $C_{44}(T)$:

$$C_{44}(T) = C_{44}^0(T - T_0^\sigma)/(T - T_0^e), \tag{9}$$

which is equivalent to our Eq. (5) in the mean-field approximation. By comparing their fitted results for T_0^σ (5 K for their ultrasonic data and 70 K for their Brillouin-scattering data) with their estimate from the neutron data[10] of $T_0^e = 72$ K, they concluded that Hirotsu's model provided a good description of their Brillouin results, and suggested that the difference between the Brillouin and ultrasonic results was due to the existence of microdomains.

We find, however, that the elastic constants found from our Brillouin data are much closer to their ultrasonic results than to their Brillouin results, suggesting that the differences they found were a consequence of the indirect method of determinination of C_{44} from mixed modes necessitated by their inability to observe the weak Brillouin scattering from pure shear modes directly. Furthermore, in view of the evidence described above that the zone-center mode on the Σ_2 soft branch is A_u rather than B_{3g}, we do not believe that their interpretation is correct. We therefore conclude that the bilinear coupling of ε_4 to the zone-center mode on the soft Σ_2 branch proposed by Hirotsu *et al.*[8] is *not* the correct explanation for the C_{44} anomaly in either Rb_2ZnCl_4 or K_2SeO_4.

For $T \leq T_i$, Rehwald *et al.*[3] fit the temperature-dependent part of C_{44} to $\Delta C_{44} \propto \rho_0^{2\beta}$ and found $2\beta \sim 0.6$–0.7. Similarly, for K_2SeO_4, Hoshizaki *et al.*[27] found $2\beta = 0.68 \pm 0.06$, while for Rb_2ZnCl_4, Matsuda and Hatta[28] found $2\beta = 0.625$ and Luspin *et al.*[9] found $2\beta = 0.6 \pm 0.1$. We similarly analyzed our C_{44} data shown in Fig. 2 by extrapolating the curve for $T > T_i$ below T_i, and fitting the excess ΔC_{44} to $A(T_i - T)^{2\beta}$, yielding $2\beta = 0.66$. However, in view of the result shown in Eq. (8), the significance of all these fits is questionable since they neglect the role of the bilinear interaction term.

B. C_{55} and C_{66} elastic anomalies

1. C_{55}

Ultrasonic studies of K_2SeO_4 have shown that the elastic constant C_{55} exhibits no observable anomaly in the vicinity of T_i, but decreases dramatically with decreasing temperatures as T approaches the lock-in transition temperature T_c, and then increases slowly below T_c.[3,7,29] Our Brillouin results shown in Fig. 2 exhibit softening in the incommensurate phase very similar to the ultrasonic results, but do not extend to (or below) T_c owing to the rapid decrease in Brillouin-scattering intensity I_{55} shown in Fig. 4.

In the Landau theory, the C_{55} anomaly arises from coupling of ε_5 strain to the order parameter via the quartic coupling terms in the free energy density

$$f_c = \tfrac{1}{2}a_5\varepsilon_5(Q^3 + Q^{*3}) + g_5\varepsilon_5^2 QQ^*, \tag{10}$$

where Q is the order parameter which is the complex amplitude of the modulation wave, and a_5 and g_5 are coupling constants. In the incommensurate plane-wave approximation, Rehwald *et al.*[3,7] and Esayan and Lemanov[29] have shown that this interaction will lead to a complex elastic constant

$$\tilde{C}_{55}(\omega) = C_{55}^0 + 2g_5\rho_0^2 - \frac{9}{4}a_5\rho_0^4\left(\frac{1}{\Omega_A^2(K_i) - \omega^2 + i\omega\Gamma_A(K_i)} + \frac{1}{\Omega_\phi^2(K_i) - \omega^2 + i\omega\Gamma_\phi(K_i)}\right) \tag{11}$$

with

$$K_i = a^* - 3q_0 = 3(q_c - q_0) = a^*\delta(T), \tag{12}$$

where $q_c = a^*/3$ is the commensurate wave vector, $q_0 = (a^*/3)[1 - \delta(T)]$ is the modulation wave vector, and Ω_A, Γ_A, Ω_ϕ, and Γ_ϕ are the frequency and damping constant of the amplitudon and phason,[30] respectively. Since $\Omega_A(K_i) >> \Omega_\phi(K_i) >> \omega$, the amplitudon term and ω^2 can be dropped, and then

$$C_{55}(\omega) = (C_{55}^0 + 2g_5\rho_0^2) - \frac{9}{4}a_5^2\rho_0^4\frac{\Omega_\phi^2(K_i)}{\Omega_\phi^4(K_i) + [\omega\Gamma_\phi(K_i)]^2}, \tag{13}$$

$$\gamma_{55}(\omega) = \gamma_{55}^0 + \frac{9}{4}\frac{q^2}{\rho_m}a_5^2\rho_0^4\frac{\Gamma_\phi(K_i)}{\Omega_\phi^4(K_i) + [\omega\Gamma_\phi(K_i)]^2}, \tag{14}$$

in which $\Omega_\phi^2(K_i) = \frac{1}{2}\Lambda_x K_i^2$. [$\Lambda_x$ and $\delta(T)$ have been determined by inelastic neutron scattering.[10]] The continuous decrease of K_i from $0.07a^*$ at T_i to $0.02a^*$ at T_c causes $\Omega_\phi(K_i)$ to decrease similarly, which in turn causes the decrease of C_{55}.

Rehwald and Vonlanthen[7] showed that Eq. (13), neglecting the g_5 term, produced a good fit to their ultrasonic C_{55} data except for the temperature region just above T_c, where the incommensurate plane-wave approximation is known to be inappropriate, and the modulation wave is better described as a soliton lattice.[30] Dvorak and Hudak[31] computed the temperature dependence of C_{55} in the soliton lattice regime and found that the anomalous part of C_{55} is proportional to the soliton density n_s, a result anticipated by Rehwald and Vonlanthen.[7] Recently, Hebbache and Poulet[32] have extended this analysis to include the role of higher-order terms in the free energy which cause a gap in the phason dispersion curve at $q_0 - \delta a^*$.

Because our C_{55} Brillouin data do not extend down to T_c, we have not attempted to fit our results to the soliton lattice predictions, but have carried out a fit to the plane-wave results of Eq. (13). The "bare" elastic constant $C_{55}^0 = (16.0 - 0.0051T)$ (GPa) was determined from the C_{55} data in the normal phase. We then fitted Eq. (13) to the data in the incommensurate phase in which K_i and Λ_x were taken from Iizumi *et al.*,[10] and Γ_ϕ was taken from Quilichini and Currat.[33] Using the same mean-field ρ_0^2 as we used in analyzing the C_{44} data, taking $\omega = 9.9$ GHz (Brillouin frequency of the C_{55} mode at room temperature), and treating a_5 and g_5 as adjustable parameters, we obtained the best fit with $a_5 = 1.9 \times 10^{34}$ $\mathrm{g}^{-1/2}\,\mathrm{cm}^{1/2}\,\mathrm{s}^{-2}$ and $g_5 = 8.8 \times 10^{26}$ s^{-2}. Figure 7(b) shows the comparison of the calculated results of Eqs. (13) with the C_{55} experimental results. The agreement is reasonable in view of the large uncertainties of the low-temperature C_{55} data.

The deviations of the ultrasonic C_{55} data from the theoretical predictions of Eq. (13) near the lock-in transition found by Rehwald and Vonlanthen[7] and ascribed to soliton effects are also seen in the lowest-temperature points in our data as shown in Fig. 8. However, the poor precision of our C_{55} data near T_c prevented us from carrying out an analysis of these effects.

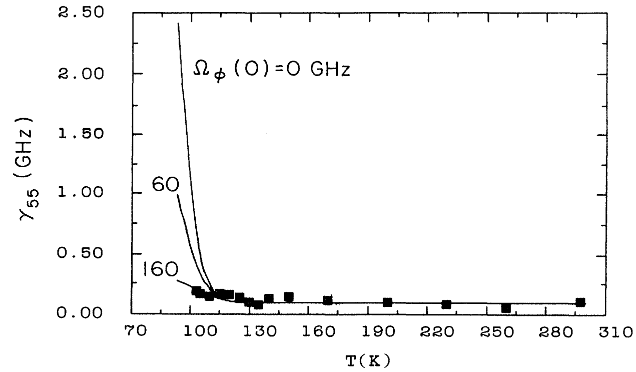

FIG. 8. Temperature dependence of the damping constant $\gamma_{55}(\omega)$. Solid lines are the calculated result of Eq. (14). The three phason gaps used were (1) $\Omega_\phi(0) = 0$, $a_5 = 1.9 \times 10^{34}$ $\mathrm{g}^{-1/2}\,\mathrm{cm}^{1/2}\,\mathrm{s}^{-2}$, $g_5 = 8.8 \times 10^{26}$ s^{-2}; (2) $\Omega_\phi(0) = 60$ GHz, $a_5 = 2.3 \times 10^{34}$ $\mathrm{g}^{-1/2}\,\mathrm{cm}^{1/2}\,\mathrm{s}^{-2}$, $g_5 = 11 \times 10^{26}$ s^{-2}; (3) $\Omega_\phi(0) = 160$ GHz, $a_5 = 4.8 \times 10^{34}$ $\mathrm{g}^{-1/2}\,\mathrm{cm}^{1/2}\,\mathrm{s}^{-2}$, $g_5 = 21 \times 10^{26}$ s^{-2}. The squares are the experimental results.

We also analyzed Eqs. (13) and (14) including a nonzero phason gap $\Omega_\phi(0)$ so that

$$\Omega_\phi^2(K_i) = \Omega_\phi^2(0) + \tfrac{1}{2}\Lambda_x K_i^2. \tag{15}$$

Phason gaps of 60 GHz (Ref. 33) and 160 GHz (Ref. 34) were considered. For the case of $\Omega_\phi = 60GHz$ the best fit was obtained with $a_5 = 2.3 \times 10^{34}$ $\mathrm{g}^{-1/2}\,\mathrm{cm}^{1/2}\,\mathrm{s}^{-2}$ and $g_5 = 11 \times 10^{26}$ s^{-2}, and for $\Omega_\phi(0) = 160$ GHz with $a_5 = 4.8 \times 10^{34}$ $\mathrm{g}^{-1/2}\mathrm{cm}^{1/2}$ s^{-2} and $g_5 = 21 \times 10^{26}$ s^{-2}. The calculated results of Eq. (13) for these two cases are essentially identical with the result shown in Fig. 7(b) calculated by using a gapless phason.

The theoretical predictions for the $\gamma_{55}(\omega)$ damping constant anomaly of Eq. (14) with $\Omega_\phi(0) = 0, 60$, and 160 GHz are plotted in Fig. 8. In contrast to the insensitivity of $C_{55}(\omega)$ to $\Omega_\phi(0)$, $\gamma_{55}(\omega)$ is very different for different phason-gap values. It is clear from Fig. 8 that the $\gamma_{55}(\omega)$ anomaly near T_c can be largely suppressed by a phason gap of $\Omega_\phi(0) \geq 100$ GHz. Although we were not able to follow the C_{55} mode close enough to T_c to reliably evaluate $\Omega_\phi(0)$, a comparison of our data with the theoretical results suggests a phason gap ≥ 100 GHz, a result which is consistent with our previous study of the C_{33} anomaly.[6]

2. C_{66}

Of the three principal transverse elastic constants, C_{66} shows the simplest temperature dependence. It only exhibits a slight change of slope at T_i as shown in Fig. 2. This anomaly can be described by the interaction with the order parameter through a quartic coupling term $g_6\varepsilon_6^2 QQ^*$. In the lowest-order approximation, the C_{66} elastic constant is given by

$$C_{66}(T) = C_{66}^0 + 2g_6\rho_0^2. \tag{16}$$

Taking the "bare" elastic constant $C_{66}^0 = (17.6 - 0.0079T)$ (GPa) obtained from the data in the normal phase above T_i, we fitted Eq. (16) to the C_{66} data points below T_i. The best fit gave $g_6 = -5.6 \times 10^{26}$ s^{-2}, in which, again, the mean-field ρ_0^2 was used. A comparison between the calculated results and the experimental data is shown in Fig. 7(c).

C. Transverse acoustic asymmetries

One of the surprising phenomena predicted to occur in incommensurate crystal phases is a breaking of the usual symmetry of the velocities of transverse acoustic waves under interchange of the propagation and polarization directions: $V_{ij} \neq V_{ji}$. Experimental evidence for such asymmetries has been reported for $BaMmF_4$,[14] $RbH_3(SeO_3)_2$,[15] and quartz.[16]

Poulet and Pick[35,36] analyzed the dynamical matrix for acoustical phonons and phasons in K_2SeO_4 and showed that phasons can only couple to transverse acoustic phonons with propagation vector **q** perpendicular to the modulation axis (the *a* axis in *Pnam*) and displacement **u** along the modulation axis. This result predicts that the sound velocities for transverse acoustic modes polarized along **a** will be shifted by the phason coupling, leading to a splitting for the pairs of C_{55} or C_{66} (but not C_{44}) modes, which increases as the temperature decreases below T_i. The same conclusion was found by Dvorak and Esayan[37] and by Lemanov *et al.*[38] from symmetry arguments. Lemanov *et al.* concluded, however, that the asymmetries due to this effect are too small to observe, since they found no evidence for asymmetries in their ultrasonic experiments on K_2SeO_4, Rb_2ZnCl_4, and $(NH_4)_2BeF_4$. They suggested that the previously reported asymmetries[14–16] must have a different origin, possibly related to the piezoelectric effect. Scott[39] proposed that the result $V_{ij} \neq V_{ji}$ may occur in incommensurate crystals with screw axes, in which the solitons can produce chiral strain fields that break the usual elastic symmetry.

Gooding and Walker[40–42] analyzed the dynamics of phasons and sound waves in K_2SeO_4 in the incommensurate phase including phason damping. They found that the K_2SeO_4 inelastic-neutron-scattering data reported by Quilichini and Currat,[33] whose damped-harmonic-oscillator analysis suggested a nonzero phason gap in the incommensurate phase, may also be explained by using a coupled phason sound-wave theory in which the phasons are gapless.[42] Therefore, whether or not the phasons in K_2SeO_4 are intrinsically gapless is still uncertain. From their analysis of the coupling effects of transverse acoustic waves with phasons, they found that the coupling with gapless phasons would cause transverse asymmetries in velocity or damping or both, whereas when the phason is not gapless, for sufficiently low-frequency (< 1GHz) transverse acoustic waves there would be no transverse asymmetry.

To further investigate the possibility of transverse acoustic asymmetries in K_2SeO_4, we studied all six pure transverse acoustic modes propagating along the three crystal axes. Within our experimental accuracy, we were not able to observe any acoustic asymmetric behavior for the pairs of transverse modes under interchange of their propagation and polarization directions as shown in Figs. 2 and 3. Although the lack of asymmetry may be due to the fact that the frequencies of the modes measured by Brillouin scattering are beyond the low-frequency regime as discussed by Gooding and Walker,[42] we note that Rehwald *et al.*[3] measured the transverse modes in K_2SeO_4 in their ultrasonics experiments using all possible combinations of polarization and propagation directions and found no inconsistencies, although they were not explicitly looking for asymmetry.

V. SUMMARY

Brillouin-scattering spectra of the six pure transverse acoustic modes of K_2SeO_4 have been measured and analyzed. We found that C_{44} shows anomalies both above and below T_i and C_{55} shows an anomaly near T_c, both being very similar to the ultrasonics result.[3] No attenuation anomalies were observed in our experiments, and no asymmetries were observed under interchange of the propagation and polarization directions within the accuracy of our experiments.

A bilinear coupling between the ε_4 strain and the lowest-frequency B_{3g} optical mode was invoked to explain the C_{44} anomaly, using the observed temperature dependence of the B_{3g} mode found from our Raman experiments as input. The calculation produced excellent agreement with the data, although the origin of the B_{3g} optical mode softening has not yet been explained. The C_{55} anomaly was analyzed on the basis of coupling of the ε_5 strain to the cube of the order parameter, within the plane-wave approximation. The damping of this mode indicates that the phason gap is > 100 GHz.

ACKNOWLEDGMENTS

We thank M.B. Walker for very helpful discussions concerning the theory of transverse acoustic modes in incommensurate crystals and N. Lenain for sample preparation. We also acknowledge helpful conversations with W. Rehwald, S. Esayan, V. Dvorak, and J. Axe. This research was supported by the U.S. National Science Foundation under Grant Nos. DMR-8614168 and DMR-9014344. Collaboration between City College, CUNY and the University P. and M. Curie, Paris was supported by the Scientific Affairs Division of NATO through Grant No. 86-0283.

*Present address: Dept. of Physics, Arizona State University, Tempe, AZ 85287.

[1] T. Yagi, M. Cho, and Y. Hidaka, J. Phys. Soc. Jpn. **46**, 1957 (1979).
[2] M. Cho and T. Yagi, J. Phys. Soc. Jpn. **50**, 543 (1981).
[3] W. Rehwald, A. Vonlanthen, J.K. Kruger, R. Wallerius, and H.G. Unruh, J. Phys. C **13**, 3823 (1980).
[4] G. Hauret and J.P. Benoit, Ferroelectrics **40**, 1 (1982).
[5] Y. Luspin, G. Hauret, A.M. Robinet, and J.P. Benoit, J. Phys. C **17**, 2203 (1984).
[6] G.Li, N. Tao, L.V. Hong, H.Z. Cummins, C. Dreyfus, M. Hebbache, R.M. Pick, and J. Vagner, Phys. Rev. B **42**, 4406 (1990).
[7] W. Rehwald and A. Vonlanthen, Solid State Commun. **38**, 209 (1981).
[8] S. Hirotsu, K. Toyota, and K. Hamano, J. Phys. Soc. Jpn. Lett. **46**, 1389 (1979).
[9] Y. Luspin, M. Chabin, G. Hauret, and F. Gilletta, J. Phys. C **15**, 1581 (1982).
[10] M. Iizumi, J.D. Axe, G. Shirane, and K. Shimaoka, Phys. Rev. B **15**, 4392 (1977).
[11] M. Wada, A. Sawada, Y. Ishibashi, and Y. Takagi, J. Phys. Soc. Jpn. **42**, 1229 (1977).
[12] N.E. Massa, F.G. Ullman, and J.R. Hardy, Phys. Rev. B **27**, 1523 (1983).
[13] M.S. Haque and J.R. Hardy, Phys. Rev. B **21**, 245 (1980); H.M. Lu and J.R. Hardy, *ibid.* **42**, 8339 (1990).
[14] I.J. Fritz, Phys. Lett. **51A**, 219 (1975).
[15] S.K. Esayan, V.V. Lemanov, N. Mamatkulov, and L.A. Shuvalov, Kristallografiya **26**, 1086 (1981) [Sov. Phys. Crystallogr. **26**, 619 (1981)].
[16] B. Berge, G. Dolino, M. Vallade, M. Boissier, and R. Vacher, J. Phys. (Paris) **45**, 715 (1984).
[17] W.K. Lee, H.Z. Cummins, R.M. Pick, and C. Dreyfus, Phys. Rev. B **37**, 6442 (1988).
[18] S. Kudo and T. Ikeda, J. Phys. Soc. Jpn. **50**, 3681 (1981); Jpn. J. Appl. Phys. **19**, L45 (1980).
[19] W.K. Lee and H.Z. Cummins, Phys. Rev. B **39**, 4457 (1989).
[20] W.P. Mason, Phys. Rev. **69**, 173 (1946).
[21] E.M. Brody and H.Z. Cummins, Phys. Rev. Lett. **21**, 1263 (1968).
[22] W. Rehwald, Adv. Phys. **22**, 721 (1973).
[23] J.C. Le Guillou and J. Zinn-Justin, Phys. Rev. Lett. **39**, 95 (1977).
[24] J.C. Le Guillou and J. Zinn-Justin, Phys. Rev. B **21**, 3976 (1980).
[25] Z.Y. Chen, Phys. Rev. B **41**, 9516 (1990).
[26] V. Katkanant, P.J. Edwardson, and J.R. Hardy, Phase Trans. **15**, 103 (1989).
[27] H. Hoshizaki, A. Sawada, Y. Ishibashi, T. Matsuda, and I. Hatta, Jpn. J. Appl. Phys. **19**, L324 (1980).
[28] T. Matsuda and I. Hatta, J. Phys. Soc. Jpn. **48**, 157 (1980).
[29] S.K. Esayan and V.V. Lemanov, Izv. Akad. Nauk SSSR, Ser. Fiz. **47**, 591 (1985).
[30] A.D. Bruce and R.A. Cowley, J.Phys. C **11**, 3609 (1978).
[31] V. Dvorak and O. Hudak, Ferroelectrics **46**, 19 (1982).
[32] M. Hebbache, Phys. Rev. B **43**, 3228 (1991); M. Hebbache and H. Poulet, J. Phys. Condens. Matter **3**, 1071 (1991).
[33] M. Quilichini and R. Currat, Solid State Commun. **48**, 1011 (1983).
[34] B. Topic, U. Haeberlen, and R. Blinc, Phys. Rev. B **40**, 799 (1989).
[35] H. Poulet and R.M. Pick, J. Phys. C **14**, 2675 (1981).
[36] R.M. Pick (unpublished).
[37] V. Dvorak and S.K. Esayan, Solid State Commun. **44**, 901 (1982).
[38] V.V. Lemanov, S.Kh. Esayan, and A. Karaev, Fiz. Tverd. Tela (Leningrad) **28**, 1683 (1986) [Sov. Phys. Solid State **28**, 931 (1986)].
[39] J.F. Scott, Ferroelectrics **66**, 11 (1986).
[40] M.B. Walker and R.J. Gooding, Phys. Rev. B **32**, 7412 (1985).
[41] R.J. Gooding and M.B. Walker, Phys. Rev. B **35**, 6831 (1987).
[42] R.J. Gooding and M.B. Walker, Phys. Rev. B **36**, 5377 (1987).